Mechanical performance and anisotropic analysis of rubberised 3D printed concrete incorporating PP fibre

Authors: Xin Lyu[1], Mohamed Elchalakani[1], Xiangyu Wang[2], Junbo Sun[3,4*], Bo Huang[5], Mohamed Saafi[6], Binrong Zhu[7], Ziqing Wei[8], Yufei Wang[9]

[1] School of Engineering, Civil, Environmental and Mining Engineering, The University of Western Australia, 35 Stirling Highway, Perth, WA 6009, Australia
[2] School of Civil Engineering and Architecture, East China Jiao Tong University, Nanchang 330013, China;
[3] Institute for Smart City of Chongqing University in Liyang, Chongqing University, Jiangsu 213300, China;
[4] School of Civil Engineering, Chongqing University, Chongqing 400045, China;
[5] School of Civil Engineering, Hunan University of Science and Technology, Xiangtan, 411201, China;
[6] Department of Engineering, Lancaster University, Lancaster, LA1 4YR, UK;
[7] College of Civil Engineering, Nanjing Forestry University, Nanjing, Jiangsu 210037, China;
[8] School of Civil Engineering, Tsinghua University, Beijing, 100084, China;
[9] School of Design and Built Environment, Curtin University, Perth, WA 6102, Australia
* Corresponding Author: Junbo Sun, E-mail address: tunneltc@gmail.com;

Abstract

The research investigates the effects of substituting sand with rubber particles derived from waste tyres—up to 40% by volume—and the inclusion of Polypropylene (PP) fibres. Unlike steel fibres, which can cause operational challenges and surface irregularities in the printing process, PP fibres' flexibility integrates well within the concrete matrix. This integration ensures smooth extrusion and a high-quality surface finish, enhancing the printability of the concrete. The study's findings reveal that including rubber particles and PP fibres impacts the concrete's properties, showing a general decline in compressive and flexural strengths as the rubber content increases. Nevertheless, the PP fibre-enhanced mixtures maintain sufficient structural strength, demonstrating an anisotropic compressive strength above 30 MPa and a flexural strength of 4 MPa. These results underscore the feasibility of using rubberised 3D-printed concrete with PP fibres in sustainable construction practices, aligning with standards (ACI 318:2018) and contributing to eco-friendly and innovative construction methodologies.

Keywords: 3D concrete printing; rubberised concrete; PP fibres; anisotropic strength; failure mode

1. Introduction

The construction industry is increasingly committed to sustainable and eco-friendly practices to mitigate its environmental footprint. One promising avenue is using recycled materials, such as rubber particles from waste tyres and Polypropylene (PP) fibres, representing a significant stride toward ecological responsibility. Rubber is a versatile and durable material that has been widely used in various applications, including construction (Liu, Setunge, and Tran 2022;

Atahan and Yücel 2012; Najim and Hall 2012). In recent years, the use of crumb rubber (CR) as an aggregate in building materials, such as plasters, mortars, and concrete, has gained widespread popularity (Elchalakani 2015; Raffoul et al. 2016; Pierce and Blackwell 2003). The disposal of rubber waste from car tires is a significant environmental challenge due to its chemical and physical durability, which makes environmentally friendly disposal difficult (Elchalakani 2015). Using recycled tire rubber in concrete provides a sustainable alternative to traditional construction methods by promoting the reuse of waste materials and reducing the consumption of natural resources (Liu, Setunge, and Tran 2022; Holmes, Browne, and Montague 2014; Saberian et al. 2019). Incorporating recycled tire rubber in concrete offers a sustainable alternative to traditional construction methods and promotes the reuse of waste materials. The use of the appropriate amount of rubber has been shown to improve the mechanical and physical properties of the resulting material (Ul Aleem et al. 2022; Pham, Elchalakani, et al. 2018; Lai et al. 2022; Levchenko and Shitikova 2024). When added to concrete, rubber particles enhance the flexibility, durability, and toughness of the final product (Pham, Zhang, et al. 2018; Zhou et al. 2023). These characteristics make the material more resistant to cracks, abrasion, and impact, leading to longer-lasting and low-maintenance structures (Pham et al. 2019; Pan et al. 2022; He et al. 2024). Using waste tire rubber in concrete is sustainable, reducing the use of sand and gravel and thus conserving natural resources. It also addresses the issue of tire waste, aligning with eco-friendly practices by lowering the carbon footprint of construction materials (Sambucci, Biblioteca, and Valente 2023; Pang et al. 2024; Liu, Cui, et al. 2021).

Various fibres like PP (P. Nuaklong 2020; Khan and Ayub 2022), Polyethylene (PE) (Antarvedi, Banjara, and Singh 2023), Polyvinyl Alcohol (PVA) (Said et al. 2021), and steel (Jain and Negi

2021) are employed to enhance the material properties of concrete in construction, each with its own set of advantages and limitations. PP fibres, in particular, are celebrated for their chemical resistance and durability, significantly enhancing concrete's tensile strength and resistance to cracking without adding much weight (Qiu et al. 2020; Yang et al. 2022; Singh et al. 2023). They disperse evenly throughout the concrete, providing reinforcement especially beneficial in environments with extreme weather, where durability against constant stress is crucial. Additionally, PP fibres improve the concrete's resistance to chemical and environmental damage, which is vital for structures exposed to harsh substances like salt water or acids, thereby reducing maintenance needs (Alyousef 2021; Feng et al. 2022; Sun, Lin, et al. 2021). While PE fibres also offer chemical and moisture resistance, they might not match the strength enhancements provided by other fibres. PVA fibres excel in bonding with concrete, improving tensile strength and crack resistance, yet they come with higher costs and potential water absorption issues (Liu, Wang, et al. 2021; Xiao et al. 2023; Sun, Wang, et al. 2022). Steel fibres significantly boost concrete's strength and structural integrity but can complicate the mixing and placement process and are prone to corrosion, impacting long-term durability (Mujalli et al. 2022; Long et al. 2023; Sun, Wang, Zhang, et al. 2021). In contrast, PP fibres present a balanced solution, enhancing mechanical properties and durability while mitigating the environmental impact by reducing the need for repairs and replacements, making them an increasingly popular choice in sustainable construction practices.

3D concrete printing is a relatively new technology that involves using specialized machines to print layers of concrete to create three-dimensional structures (Petrovic et al. 2010; Sun, Aslani, et al. 2021; Sun, Wang, Liu, et al. 2021). This innovative technology has several advantages over traditional concrete construction methods. One of the primary advantages of 3D printing concrete is its ability to reduce construction times significantly. Traditional construction methods require formwork and manual labour to pour and shape concrete, which can be time-consuming and labour-intensive (Singh et al. 2022). In contrast, 3D printing can produce complex structures layer by layer in a fraction of the time it would take using traditional methods. This not only saves time but also reduces labour costs and minimizes the risk of human error (Nebrida 2022). 3D printing concrete offers another significant benefit: the potential to cut costs. Traditional construction methods often involve hefty expenses due to the need for formwork, labour, and transportation, particularly with large or intricate structures. In contrast, 3D printing can diminish material waste and make the construction process more efficient, leading to potential savings. This method also allows designers and engineers to craft custom shapes and structures, which might be more economical and efficient than conventional designs (Singh, Colangelo, and Farina 2023; Panda). Beyond cost reduction, 3D printing in concrete construction also contributes to environmental sustainability. By using only the necessary amount of concrete, it minimizes waste, thereby lessening the environmental footprint of construction projects (Alami et al. 2023; Panda). 3D concrete printing reduces waste by using only the required amount of concrete, minimizing material waste, and lowering the environmental impact of construction projects. This technology contributes to sustainability by optimizing material usage and reducing the carbon footprint of construction activities (Chengxiu Jia 2022; Sun et al. 2023; Zhu et al. 2023).

The study explores the impact of rubber particle inclusion on the fresh and hardened engineering properties of 3D Printed Fibre-Reinforced Concrete (3DPFC). A thorough set of tests, including flowability, printability, and mechanical properties such as compressive and flexural strength in different directions, was conducted at ambient conditions. These tests utilised concrete modified by rubber particles, with rubber content varying from 0% to 40% as a volume replacement. The Global Warming Potential (GWP) of each mixture was calculated to assess its environmental impact. The failure mechanisms of the rubber-modified 3DPFC were scrutinised through microstructural analysis and Digital Image Correlation (DIC) techniques.

2. Experimental programs

2.1 3D Printing System

Figure 1 shows the gantry 3D printing system used in this study. This device consists of a gantry system with dimensions of (2.5×2.5×2m). The printing head was mounted with a screw-type extrusion head, whose speed can be varied. The gantry can move at a maximum speed of 10cm/s. A stereolithographic file, also known as G-Code file, is used to input the commands for printing. To increase the uniformity and extrudability of the printing materials, they were first combined in a conventional mixer before being transferred to the print head and then again in the material container. The layers of 3D objects were formed by moving the print head simultaneously in the X, Y, and Z directions.

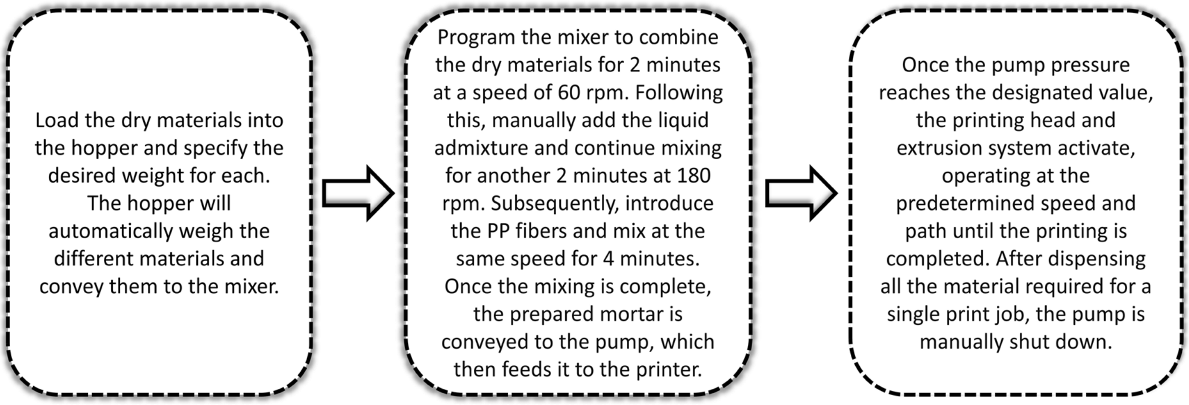

(a)

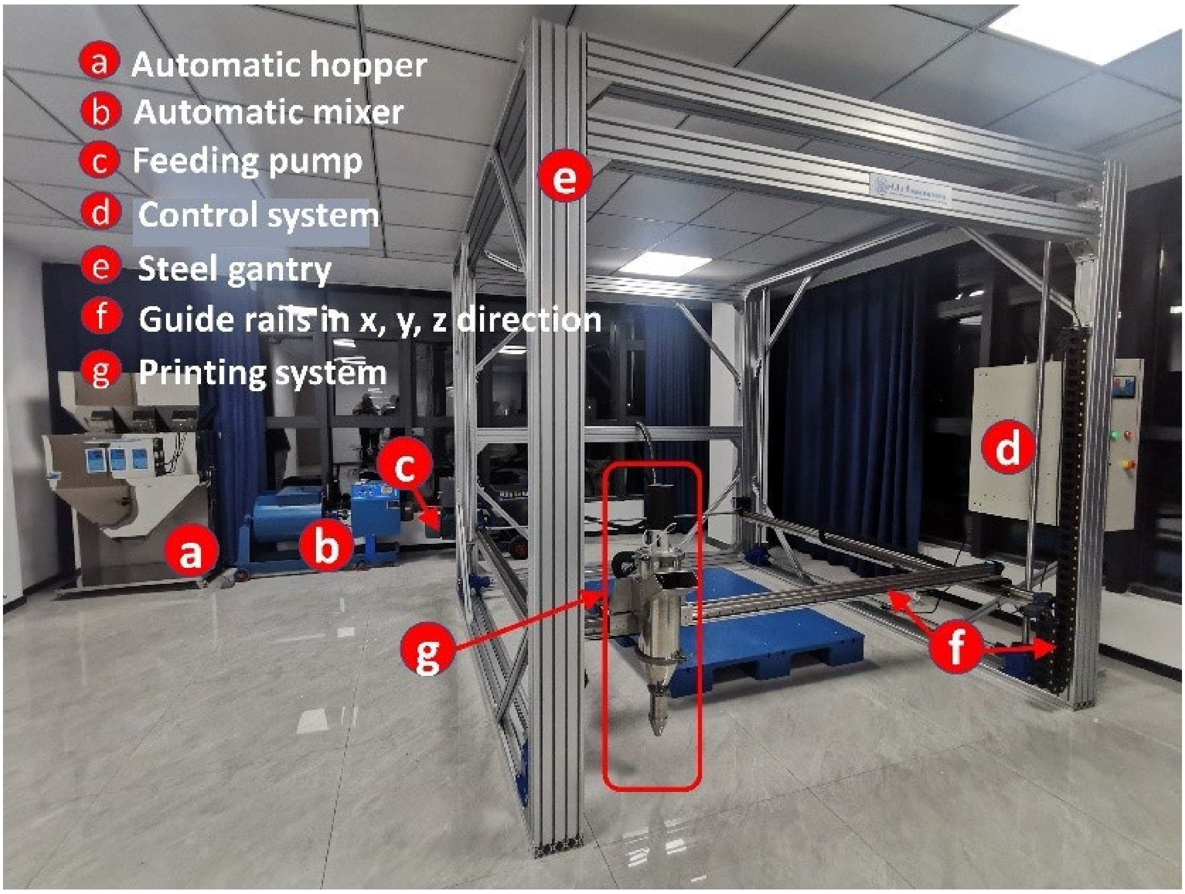
a Automatic hopper
b Automatic mixer
c Feeding pump
d Control system
e Steel gantry
f Guide rails in x, y, z direction
g Printing system
a
b
c
d
e
f
g

(b)

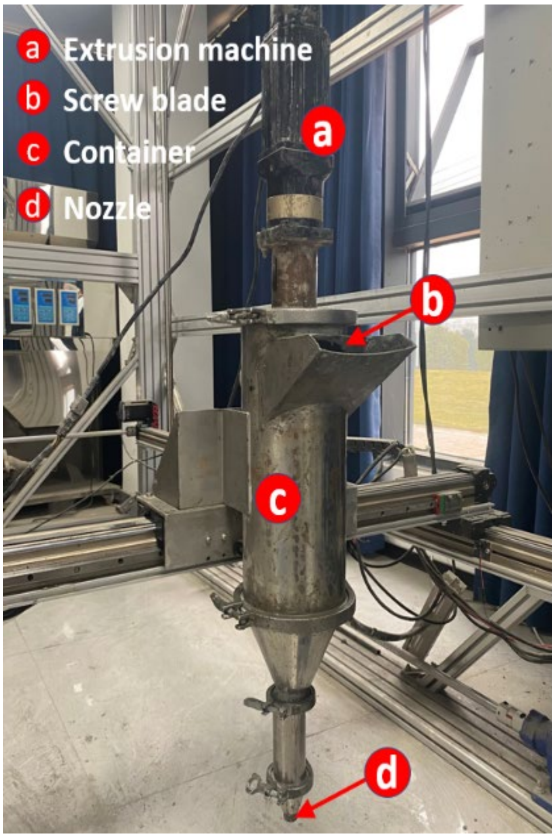
a Extrusion machine
b Screw blade
c Container
d Nozzle
a
b
c
d

(c)

Figure 1: 3D gantry printer (a) operation procedure (b) photography of 3d printer (c) photography of printing head

2.2 Materials and mix proportions

In this research, various samples were crafted using different raw materials: type II 42.5 ordinary Portland cement (OPC), grade 955 silica fume (SF), fine quartz sand characterised by a maximum dimension of 300 μm and an average size of 100 μm, 6 mm length chopped PP fibres, rubber particles (RP), hydroxypropyl methylcellulose (HPMC) with a viscosity benchmark of 200000 mPa·s, powdered polycarboxylate-based superplasticiser (SP), nano-clay (NC), sodium gluconate (SG), and standard tap water. The mixture proportions (see Table 1) include three different RP contents (based on the volume fraction of silica sand) - specifically 0%, 20%, and 40%. PP fibres were introduced to mitigate shrinkage and bolster the matrix. Their physical and mechanical attributes are outlined in Table 2. The chemical compositions of both OPC and SF can be found in Table 3. Both RP and quartz sand were employed as fine aggregates. The RP particles were observed to be relatively larger than quartz sand grains. Specifically, 120-mesh RP (equivalent to 0.125 mm) derived from recycled tires was chosen to partially supplant quartz sand. The tire rubber powder is a polymer organic matter with a non-polar surface. In contrast, the cement matrix is an inorganic matter with a polar surface. To promote the bonding properties between them, water washing and infiltration were used to modify the surface of the rubber powder. The surface of the treated rubber powder was shown in Figure 2. Figure 3 presents scanning electron micrographs of the water-washed rubber particles. The chemical detection content of rubber powder is shown in Table 4. The integration of HPMC, SP, and NC targeted achieving optimal workability and thixotropy for the freshly printed filament. Concurrently, SG, an analytical reagent, acted as a retardant, modulating the setting period of the cement mortar (Chen et al. 2020). Figure 4 provides the particle size distributions of RP and quartz sand.

Table 1: Mix proportion of mixes (mass%).

Mix ID	Cement	Fly ash	Silica fume	Sand	Rubber	Hydroxypropyl methylcellulose (HPMC)	nC (Nano-clay)	PP fibre	Sodium glauconite	SP	Water
PP1.5-R0	10	12	3	8.75	0	0.02	0.1	0.27	0.01	0.1	6.5
PP2-R0	10	12	3	8.75	0	0.02	0.1	0.36	0.01	0.1	6.5
PP1.5-R20	10	12	3	7	0.66	0.02	0.1	0.27	0.01	0.1	6.5
PP2-R20	10	12	3	7	0.66	0.02	0.1	0.36	0.01	0.1	6.5
PP1.5-R40	10	12	3	5.25	1.32	0.02	0.1	0.27	0.01	0.1	6.5
PP2-R40	10	12	3	5.25	1.32	0.02	0.1	0.36	0.01	0.1	6.5

Table 2: Properties of PP fibres.

Elongation at break	Length	Diameter	Tensile modulus	Tensile strength	Melting point	density
30%	6mm	31μ m	≥3.5GPa	460MPa	160℃	0.91

Table 3 Chemical composition of OPC and SF (wt%).

Oxide	SiO_2	Al_2O_3	Fe_2O_3	CaO	MgO	SO_3	Na_2O	K_2O	P_2O_5	ZnO
OPC	20.10	4.60	2.80	63.4	1.30	2.70	0.60	—	—	—
SF	98.32	0.38	0.13	0.15	0.14	0.68	—	0.09	0.07	0.05

Table 4: The chemical composition of rubber (mass%)

Heating decrement	Ash content	Fe	Fibre	Sieve residue	Bulk density	Specific density
0.62%	8.75%	0.029%	0	0.014	314kg/m^3	1.02

Figure 2: Rubber powder surface

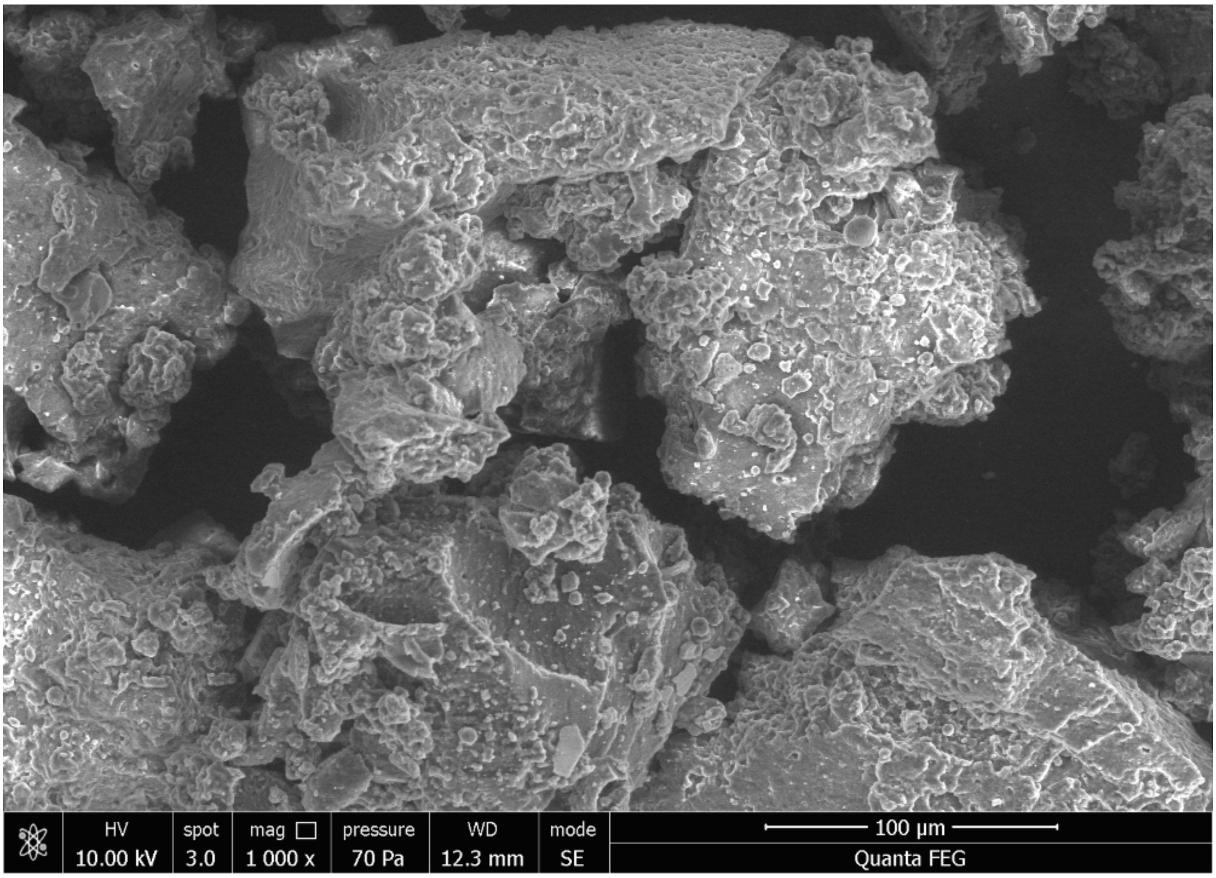

Figure 3: Scanning electronic micrographs of rubber particles.

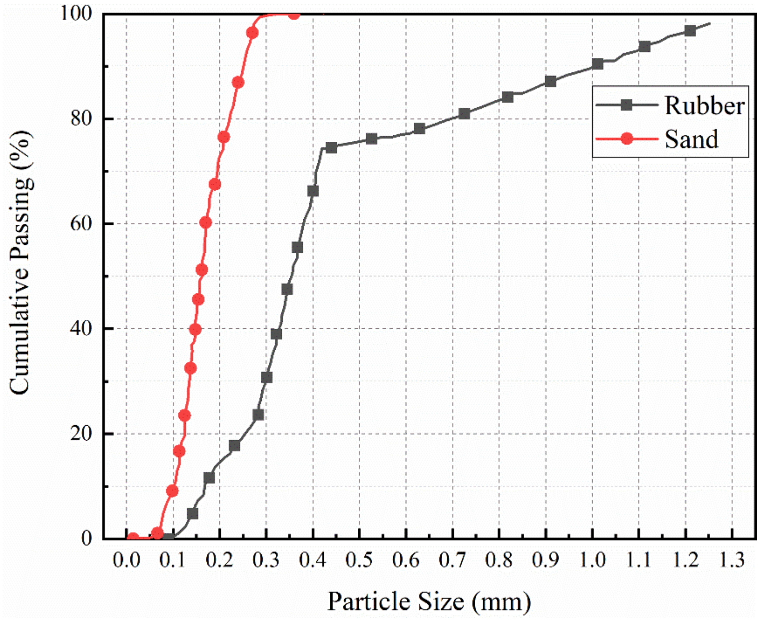

Figure 4: Particle size of sand and RP

2.3 Fresh properties

The workability of the six samples was assessed through slump flow measurements taken at various resting times. These measurements followed the GB/T 2419-2005 standards ('GB/T2419-2005, Chinese Standards, Test Method for Fluidity of Cement Mortar, Chinese Standards Association, China, 2005.'), utilising a mini-cone apparatus for the flow table tests. The dimensions of the mini cone used were as follows: a height of 60±0.5 mm, a top diameter of 70±0.5 mm, and a base diameter of 100±0.5 mm. Upon casting the fresh mortar into the mould, the table underwent 25 drops within 25±1 seconds immediately following the removal of the mini cone. The average spread diameters, ascertained in at least two directions, served as the slump flow. This procedure was reiterated at 10-minute intervals over a 60-minute duration to track the time-dependent workability of the fresh material. Workability, extrudability, and buildability were all essential for assessing the mixture's printability. Each sample group's extrudability and buildability were evaluated by 3D printing rectangular slabs of a set height.

2.4 Preparation process and print settings

The printing device used in this study consisted of two parts: the feeding system and the extrusion system. The material supply in the printing process can be selected by machine pumping or manual filling. The method of machine pumping can realise the automatic control of large flow rate and handle the high viscosity mixture. The manual filling method is ideal for printing materials with low flow rates, allowing timely adjustments to meet printing demands. For printing materials, the use of machine pumping requires higher dimensions for the rotor and stator in the stirring pump to minimize fibre interactions (friction and extrusion) that may cause excessive damage to the stirring pump. Furthermore, given the material's deformation over time and the need for precise raw material control, this study employed small-scale mixing and manual feeding. This approach ensured optimal fibre dispersion and printing performance. The dry raw materials, including rubber powder, are first mixed at a consistent rate of 1000 rpm. After this, water and SP are added, and the mixture is stirred for 3 minutes. The PP fibres and SG are then added, ensuring the fibres are properly dispersed and mixed until the mixture reaches the desired fluidity and a printable state. The printing process is shown in Figure 5, the material is transferred from the mixer to the pump and the extruder to build the printing item.

Figure 5: Printing process of PP fibre reinforced rubberised concrete

2.5 Compressive and flexural strength

To evaluate compressive and flexural strength, cubic samples with dimensions of 50 × 50 × 50 mm^3 and prismatic samples measuring 40 × 40 × 160 mm^3 were carefully sawed and polished from 3D printed slab elements of sizes 200 × 200 × 150 mm^3 and 330 × 290 × 210 mm^3, respectively. These measurements were conducted at the test ages of 28 days. Loading was applied in three orthogonal directions, F_x, F_y, and F_z, to investigate the anisotropic mechanical properties of the 3D printed samples, as illustrated in Figure 6. Compressive strength was calculated using Equation (1) in accordance with AS 1012.9-2014 (Australia 2014). Flexural performance was assessed using a three-point bending test, evaluated by Equation (2) as per AS 1012.11-2000 (Australia 2000). In Equation (1), σ_c is the compressive strength (MPa), P is the maximum applied load (N), and A is cross-section area of the tested specimen (mm^2). In Equation (2), σ_f is the flexural strength (MPa), P is the maximum applied load (N), L is the distance between supports (mm), b is the width of the specimen (mm), and d is the height of the specimen (mm). Both compressive and flexural tests were carried out using an automatic pressure-testing machine.

$$\sigma_c = \frac{P}{A} \tag{1}$$

$$\sigma_f = \frac{3PL}{2bd^2} \tag{2}$$

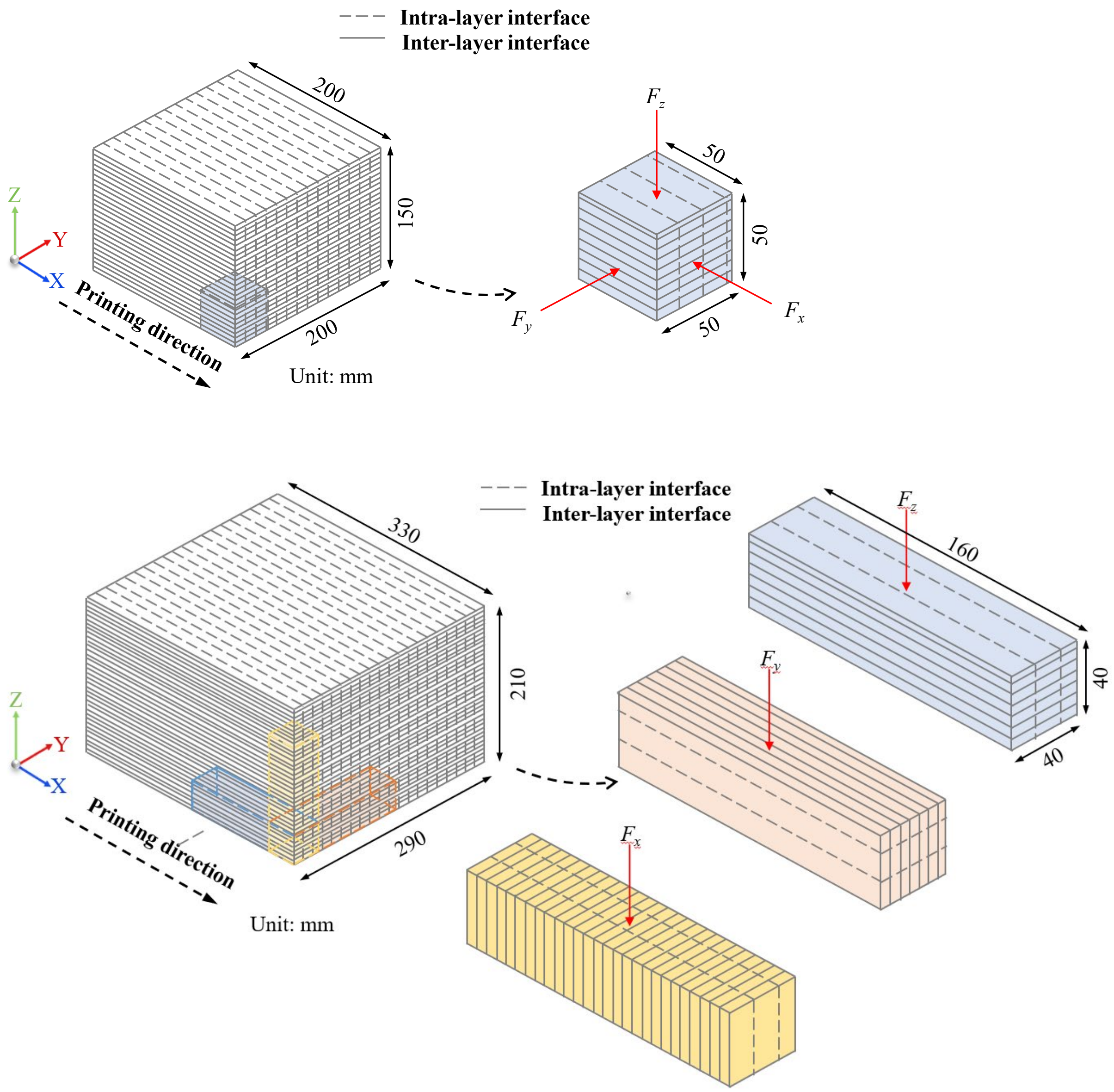

Figure. 6: Schematic diagram of samples extracted from printed samples and anisotropic loading directions of compressive strength tests (top) and flexural strength tests (bottom).

2.6 Environmental assessment

The environmental assessment refers to ISO 14040 (ISO 2006) and uses OpenLCA software.

The functional unit for this study is 1 m³ of concrete with varying proportions of raw materials. Inventory flows include inputs of raw materials, outputs of the concrete mix, and emissions to air, land, and water, sourced from the Ecoinvent v3.8 database. Waste rubber was managed as municipal waste, and its reuse contributed to the reduction of harmful solid waste incineration, thereby benefiting the environment. Based on the Ecoinvent database, this waste is processed in a municipal solid waste incinerator (MSWI). The study focuses on environmental impact indicators such as Abiotic Depletion (ADP), Acidification Potential (AP), and Global Warming Potential (GWP). The environmental impact of producing 1 m³ of concrete is analysed using the CML method (Jawad, Ghayyib, and Salman 2020), prescribed in EN15804, which characterises and normalises environmental impact indicators. Characterisation results are quantified as follows: ADP in kg antimony equivalent, AP in kg SO_2 equivalent, and GWP in kg CO_2 equivalent. These indicators are normalised by dividing the characterised results by the total equivalent emissions per year for a given geographical region. The normalisation inventory, detailing all regional emissions and resource extractions over a year, is sourced from OpenLCA software and presented in a unified unit: year.

3. Results and discussion

3.1 Fresh properties

Flowability in the examined mixtures demonstrates a positive correlation with RP content yet exhibits an inverse relationship with the presence of PP fibres (see Figure 7). PP fibres are inherently hydrophobic, increasing viscosity and internal friction within the mortar, thus reducing flowability. Conversely, the inclusion of RP enhances flowability. This observation contradicts much of the current research on rubberised concrete, where increased RP content usually leads to reduced workability (Hossain et al. 2019; Sun, Tang, et al. 2022). The improved flowability is likely due to reduced surface friction between RP and other ingredients during mixing, given the smoother texture of RP compared to sand. Additionally, the rubber particles in this research are larger than quartz sand, leading to decreased water absorption rates (Mohammed and Azmi 2011). Flowability tests were conducted at 10-minute intervals over an hour. In this study, the waiting time for the mixture in the pump should not exceed 30 minutes. Flowability ranged from 120 mm to 164 mm, satisfying practical requirements for pumping and extrusion and aligning with findings by Panda et al. (Panda and Tan 2018). The best flowability was found in a mix with 1.5% PP fibre and 40% rubber, considering factors like the printing head size, travel speed, and extrusion speed.

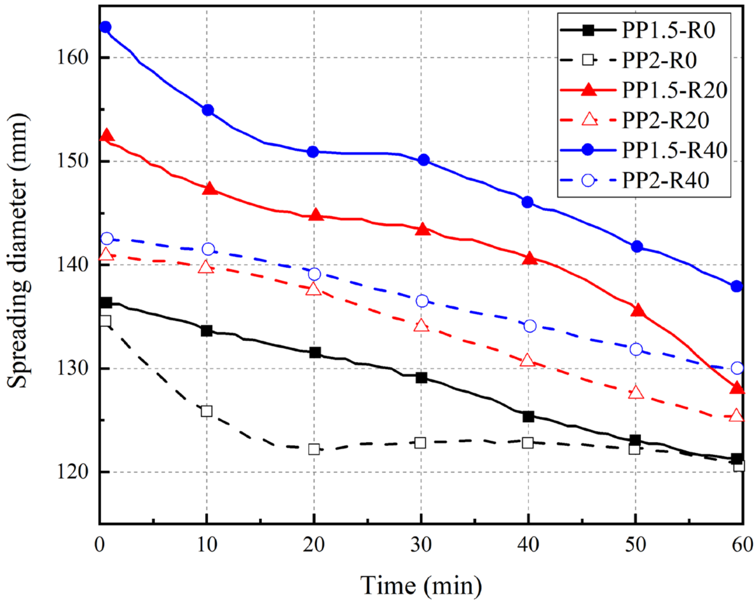

Figure 7: Spreading diameter of fresh mixtures

Extrudability refers to how easily concrete can be 3D printed during extrusion and the resulting surface quality and consistency after extrusion (Rehman and Kim 2021). Understanding extrudability is crucial for ensuring the concrete mortar can be consistently conveyed through the feed pipe and smoothly deposited via the printer's nozzle. This consistency is essential for the integrity of the construction and facilitates continuous printing. Previous research by

Hambach et al. (Hambach and Volkmer 2017) indicates that a fibre content exceeding approximately 1.5% in cement-based materials may lead to nozzle blockage. Buildability refers to the structural stability and minimal deformation of 3D-printed cement-based materials. It is influenced by the material's capacity to bear its weight during extrusion and the gravitational force exerted by subsequent layers. A strong bond between consecutive layers is essential to avoid structural failures or distortions, emphasizing the need for materials that offer excellent interlayer adherence and maintain their shape. Buildability is crucial for gauging initial structural stiffness, component integrity, and layer stability. Optimizing aggregate grading and incorporating mineral admixtures and additives can enhance buildability. For instance, adding 2% silica fume and nano clay to the cement increased construction height by 261% (Hambach and Volkmer 2017). Figure 8 illustrates the extrudability and buildability performance of various 3D-printed concrete slabs with differing mix compositions. The results show that filaments could be consistently extruded from the printing nozzle, and the completed printed structure displayed excellent shape stability. These findings set the foundation for future mechanical property evaluations, indicating that the mixtures formulated in this research, with varying rubber particle content, are suitable for further assessments.

(a) PP1.5-R0 (b) PP1.5-R20 (c) PP1.5-R40

(d) PP2-R0 (e) PP2-R20 (a) PP2-R40

Figure: 8 Extrudability and buildability of 3D printed structure for different mixtures.

3.2 Microstructure

The microstructural characteristics of the PP2-R0 and PP2-R20 samples after flexural testing were observed using the Gemini300 Scanning Electron Microscope (SEM). As depicted in Figure 9 (a), a discernibly rough texture on the side walls of the void left by PP fibre was evident, and wool flocs were embedded within the PP fibre surfaces. The wool flocs on the side wall and surface of PP fibres suggest effective chemical bonding between the PP fibres and the matrix, ensuring strong adhesion between them (Abdallah, Fan, and Cashell 2017). When the PP fibres experience tensile stress, small flocs emerge from their surface, which could combat the tension. Despite the increasing strain, the fibre maintains its connection with the matrix. This phenomenon contributes to the enhanced ductility in PP fibre-reinforced concrete. Incorporating rubber diminishes the matrix's toughness, facilitating the extraction of fibres from the matrix under tensile. Figure 9 (b) illustrates increased voids due to the extraction of PP fibres or rubber particles. There were no observable cracks or gaps at the interface between the amorphous rubber particles and the cement mortar.

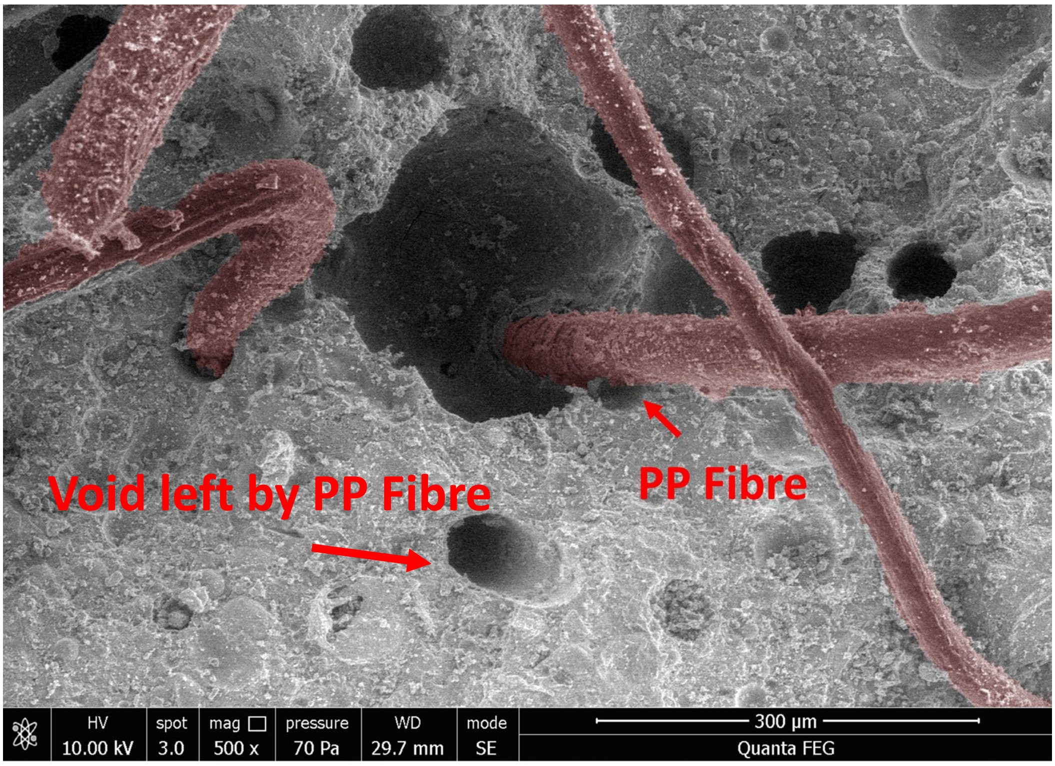

(a) PP2-R0

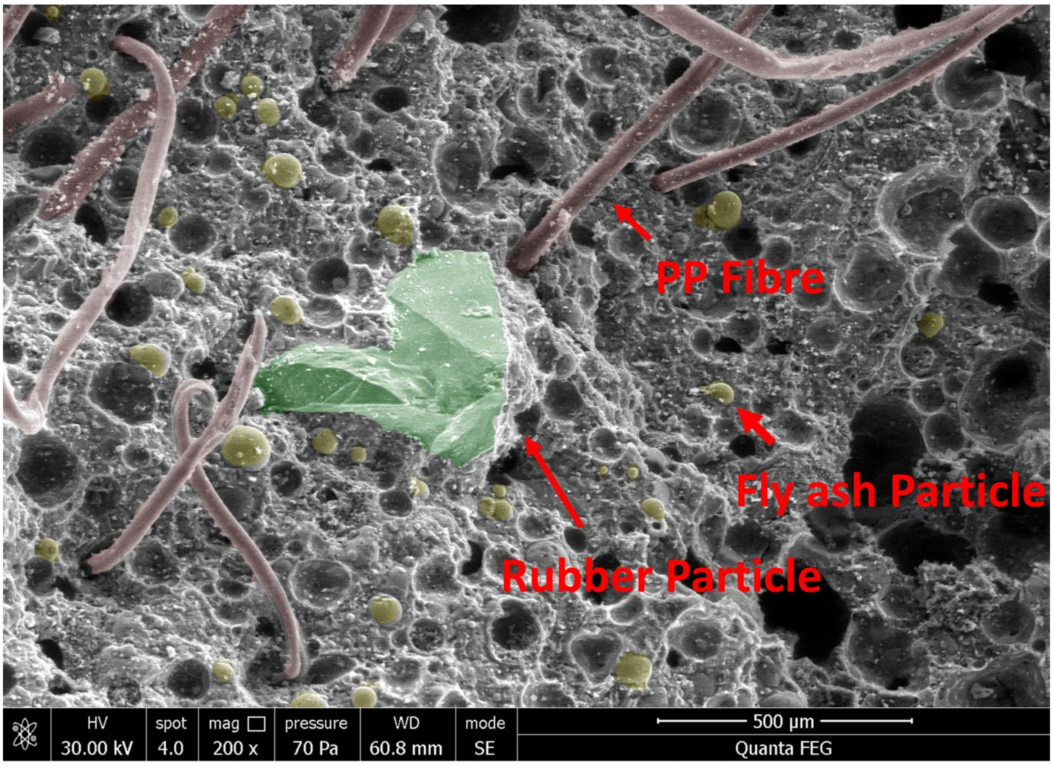

(b) PP2-R20

Figure 9: SEM images of (a) PP2-R0 and (b) PP2-R20 samples after flexural testing.

3.2 Anisotropic Compressive Strength

As indicated in Equations (3) and (4) (Yao et al. 2023), in this study, anisotropic coefficients were used to reflect the impact of printing method on the mechanical properties of materials.

$$f_{avg} = \frac{\sum_{n=1}^{i} f_{xn} + \sum_{n=1}^{i} f_{yn} + \sum_{n=1}^{i} f_{zn}}{3i} \tag{3}$$

$$I_a = \frac{\sqrt{\left(f_{x_1} - f_{avg}\right)^2 + .. + \left(f_{x_i} - f_{avg}\right)^2 + \left(f_{y_1} - f_{avg}\right)^2 + .. + \left(f_{y_i} - f_{avg}\right)^2 + \left(f_{z_1} - f_{avg}\right)^2 + .. + \left(f_{z_i} - f_{avg}\right)^2}}{f_{avg}} \tag{4}$$

$'\sum_{n=1}^{i} f_{xn}$, $\sum_{n=1}^{i} f_{yn}$, $\sum_{n=1}^{i} f_{zn}'$ represents the sum of the load in the principal load direction, $'f_{avg}'$ represent the average strength in the X, Y, and Z directions. Constant $'i'$ represents the number of tested samples for each mixture. $'I_a'$ represents the coefficient of anisotropy. For practical high-quality structural printing, it is preferable to use lower $'I_a'$ values.

Figure 10 presents the compressive test results for six mixtures. The mechanical properties of concrete with consistent PP fibre content fluctuate based on the loading direction, highlighting a pronounced mechanical anisotropy. The maximum compressive strength is exhibited in the F_x loading direction, followed by the F_y and F_z directions, corroborating prior studies (Wang et al. 2022). In this research, the X direction demonstrated superior compressive strength, exceeding the average strength by 23.71%, 23.08%, 12.15%, 21.35%, 18.74%, and 11.86%. In contrast, the Z direction displayed the weakest mechanical properties, with compressive strength values of 50.89%, 21.5%, 24.35%, 46.14%, 26.38%, and 28.76% below the average strength. This phenomenon may be attributed to the elevated internal extrusion pressure in the concrete on the F_x axis, coupled with the unavoidable water secretion during the extrusion of concrete filaments by the printing nozzle. Consequently, this slightly reduces the water-cement ratio, rendering the 3D printed concrete denser and more robust in X derection (Liu et al. 2022). In contrast, the Z-direction loading in the short-sided stacking structure shows signs of instability, a heightened risk of tipping over, and a tendency to magnify defects present in the weak inter-layer zones. Additionally, the layers of concrete were not tightly bonded. When subjected to force in the Z direction, the layers are prone to separation or sliding, resulting in structural failure. This lack of effective layer bonding contributes to the diminished compressive strength observed in the Z direction (Yao et al. 2023).

In this study, an increment of PP fibre from 1.5% to 2% was associated with a minor decline in compressive strength. This could be because samples containing 2% PP fibre content demonstrated a noticeable reduction in workability. Consequently, this leads to increased voids in the concrete matrix, resulting in a diminished compressive strength compared to samples with 1.5% PP fibre. However, based on the relevant literature, the appropriate incorporation of PP fibres into concrete can enhance the mechanical performance of 3D printable concrete (Behfarnia and Farshadfar 2013; Ding et al. 2018). However, this improvement in compressive strength is not as marked as it is in tensile properties, since the matrix's strength predominantly governs the compressive strength (Gesoglu et al. 2016).

Figure 11 exhibits that the compressive strength largely diminishes with the escalating content of rubber. This is observable in a) the average compressive strength across all three directions, b) the x direction, c) the y direction, and d) the z direction. This diminution in strength can be accredited to the inherently lower strength of CR compared to silica sand, and a weaker bonding relationship between the CR particles and the cement matrix (Pham et al. 2019). The strength decrease is more pronounced in the X direction than in the Z direction. The observed reduction in strength could be ascribed to two primary factors. First, due to the inherent softness or elasticity of the rubber particles relative to the surrounding materials, cracks tend to form quickly around these particles when subjected to load. This leads to a faster failure of the rubber-cement matrix. Secondly, owing to the deficient adhesion between the rubber and cement paste, these soft rubber particles may act similarly to voids within the concrete matrix (Alsaif et al. 2018; Gerges, Issa, and Fawaz 2018). In a dense and strong matrix like that in the x direction, cracks may propagate around the rubber, leading to failure and a noticeable decrease in strength. Conversely, in a weak and porous matrix, the rubber might diffuse stress concentration along a particular path (Strukar et al. 2018; Yu et al. 2020). This results in less evident strength reduction in the z direction and may even exhibit a marginal increase with a rubber content of 20% (see in Figure 11 d)).

Figure 12 delineates the coefficient of anisotropy, denoted by I_{ac}, for six distinct mixtures. The I_{ac} illustrates a consistent reduction as the rubber content increases. This trend can be attributed to a couple of reasons. Initially, the incorporation of rubber reduces the average strength, with this effect being more pronounced in a robust matrix and less significant in a softer matrix. This results in a reduction in directional differences, thereby decreasing Ia. Secondly, as previously highlighted, rubber, due to its softness, is easily deformed under pressure. This characteristic diminishes the intensity of stress concentration at the crack tip (Yu et al. 2020), thereby averting premature failure and offsetting defects between printing strips and layers.

Figure 13 employs DIC technology to capture the crack propagation in the PP1.5 mix with varying rubber content, loaded in the X direction. The synergistic effect of crumb rubber and PP fibres results in gradual failures rather than sudden ones. The sample with 0% rubber showed a distinct tendency for diagonal cracking upon reaching the maximum load, resulting in a shear compression failure characterized by a conical fracture pattern. Contrastingly, the introduction of CR precipitated several changes. Firstly, primary cracks appeared at 60% of the peak load, earlier than in the rubber-free mix. Secondly, the failure mode transitioned from shear compression to axial compression. Lastly, the incidence of cracks increased with escalating rubber content, with only a single main crack observable in the R0 mix but multiple in R20 and R40. This behaviour can be linked to the role of rubber particles in guiding crack growth and enhancing energy absorption. When cracks traverse rubberized concrete, the rubber particles deform significantly. This deformation absorbs part of the impact energy, reducing stress concentration at the crack's tip. This prevents early failure and enhances the material's toughness. As a result, microcracks in the material expand more gradually, allowing the primary crack to fully develop, leading to better energy dispersion and more controlled crack growth (Gerges, Issa, and Fawaz 2018).

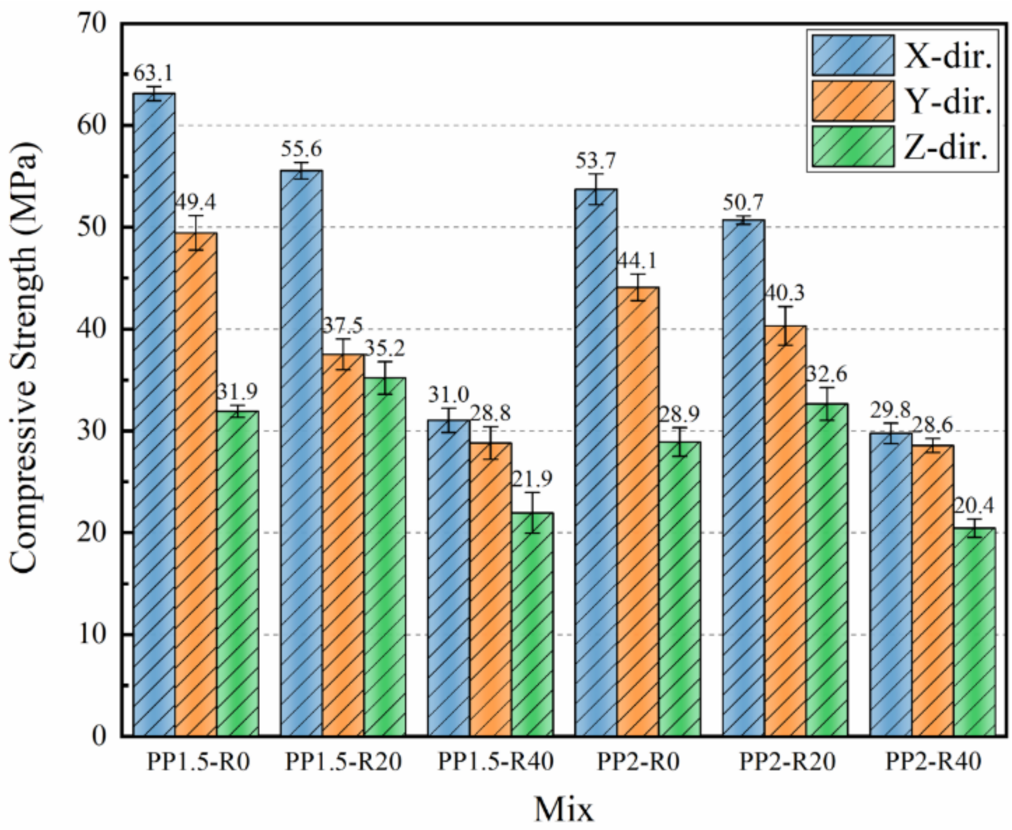

Figure 10: Compressive test results

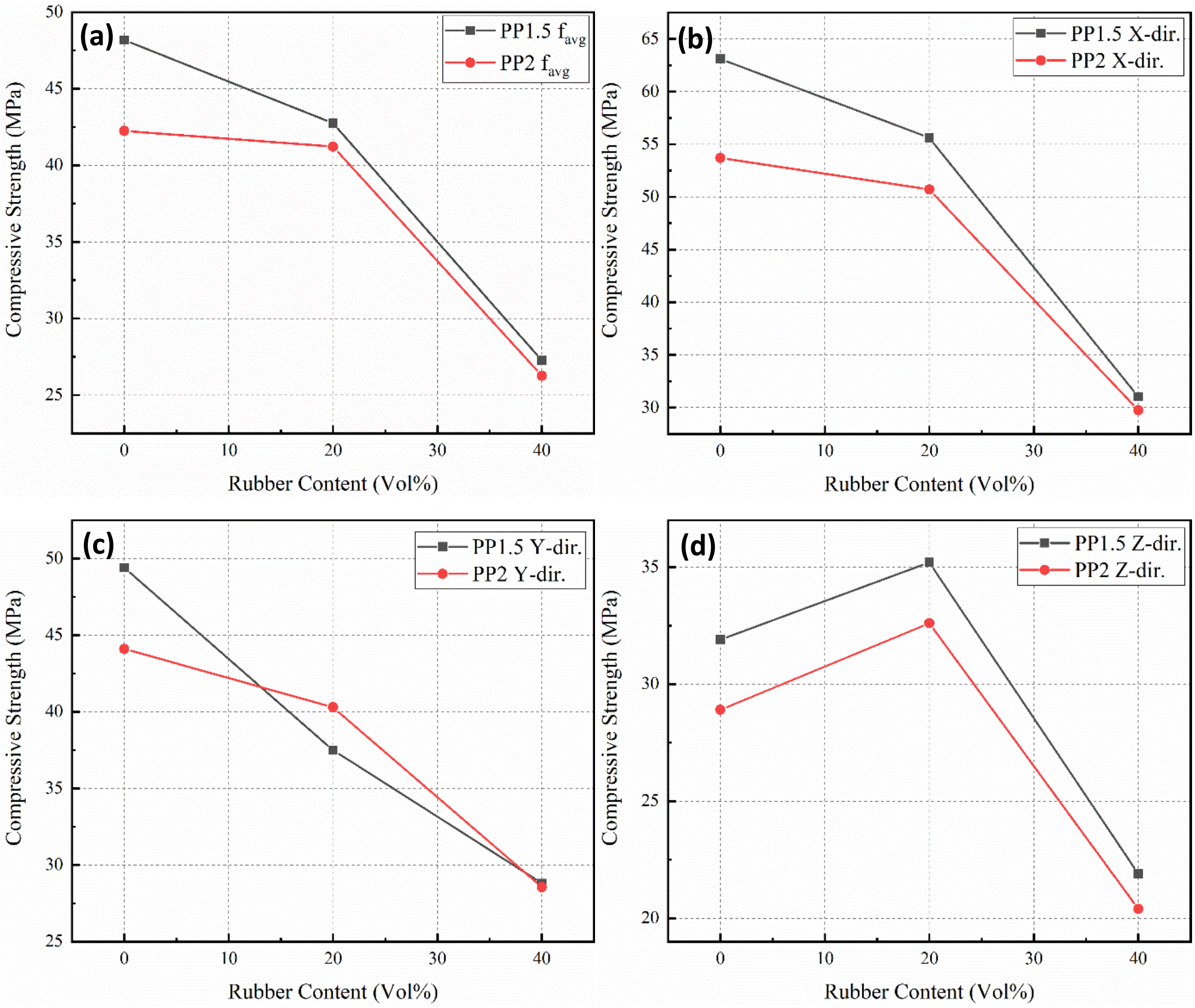

Figure 11: Compressive strength with the escalating content of rubber (a) average strength, (b) in x-dir. (c) in y-dir. (d) in z-dir.

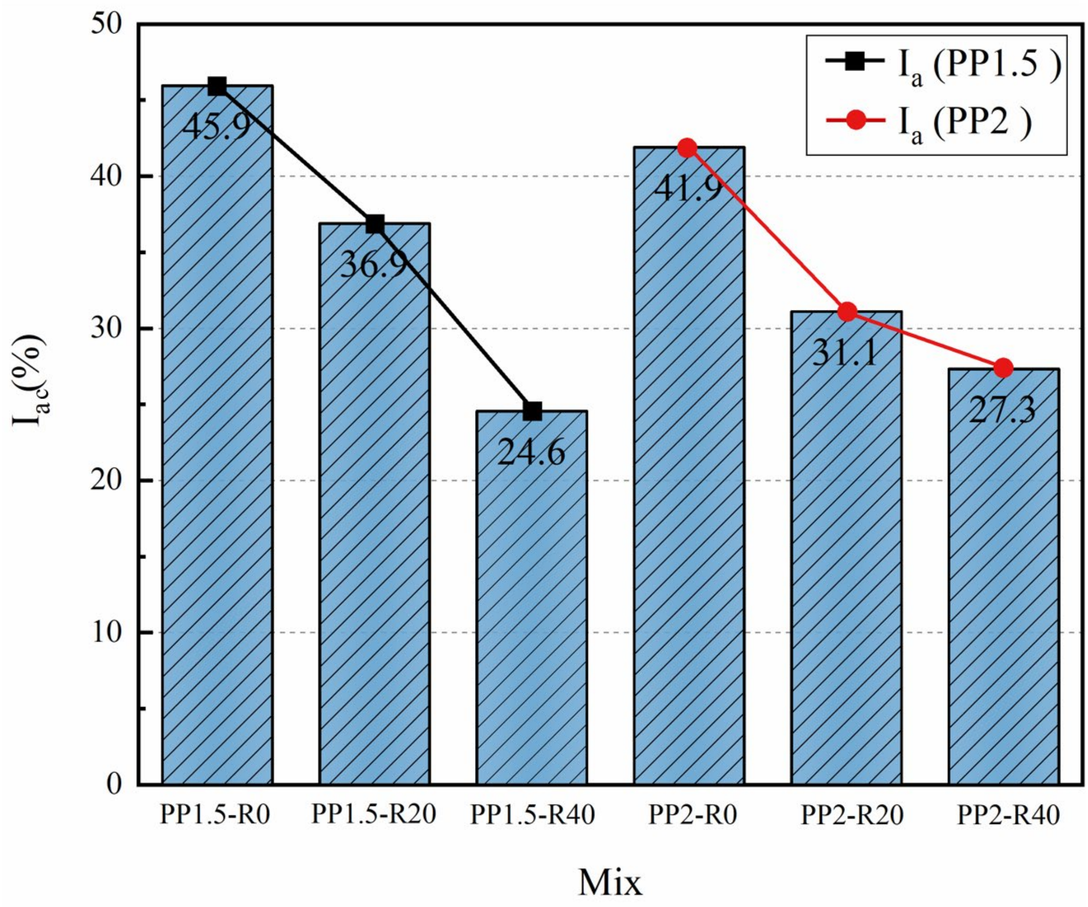

Figure 12: Coefficient of compressive anisotropy (I_{ac})

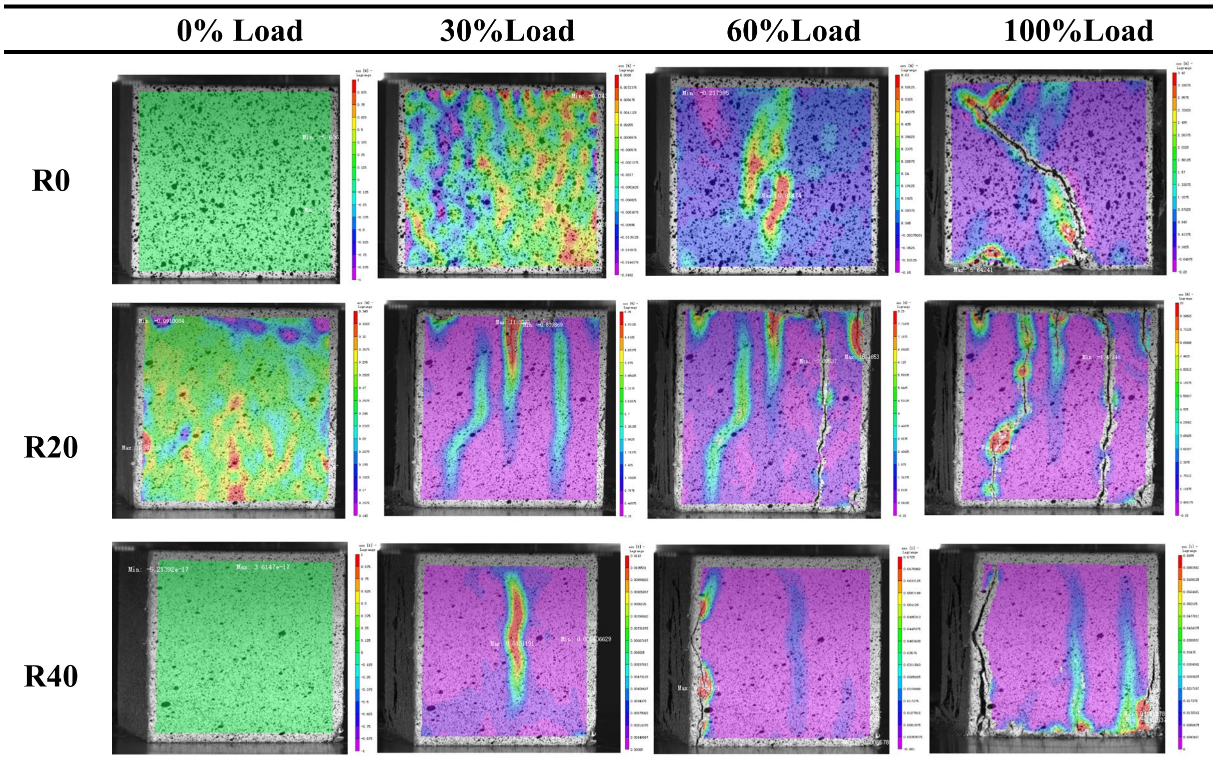

Figure 13: DIC Analysis of crack propagation with varying rubber content under X-direction loading.

3.3 Anisotropic Flexural Strength

Figure 14 illustrates the flexural strength across six different mixtures. The PP2-R0 mixture demonstrates the highest flexural strength, registering at 6.7 MPa in the Y-direction, aligning with results from Ye et al. (Ye et al. 2021). Lower flexural strength in the X-direction samples can be attributed to weak interfaces perpendicular to the principal tensile stress direction. Samples in the Z-direction display the second-highest flexural strength, while those in the Y-direction register the highest. In the Y and Z directions, samples exhibit similar interface distributions without weak interfaces in the tensile direction. The interfaces in Y-direction samples correspond to the intra-layer interfaces encountered during the 3D printing process, whereas those in the Z-direction samples relate to the inter-layer interfaces. The distinct bonding strengths of these interfaces may account for the differences in flexural strength between the Y and Z loading directions, aligning with results from Panda et al. regarding the directional dependency of the properties of 3D printing technology (Panda, Chandra Paul, and Jen Tan 2017).

Figure 15 provides an average of the flexural strength across different mixtures. The trend indicates a decrease in strength as the rubber content within the mix increases, while flexural strength improves with an increase in fibre content. The fibres' high specific surface area enhances their adhesion to the mortar, and the overlapping of fibres contributes to a synergistic effect under bending loads (Hambach and Volkmer 2017). Figure 16 presents the coefficient of anisotropy of flexural strength, denoted as I_{af}, for these six mixtures. This data suggests that rubber particle content does not significantly impact the anisotropy of the flexural properties, corroborating findings in existing literature that the inclusion of rubber particles in the mix does not create a directional bias in the material's ability to resist bending forces (Nerella, Hempel, and Mechtcherine 2019). The increase in the flexural anisotropy coefficient at PP1.5-R40 can be attributed to several factors: First, the absolute difference in flexural strength is relatively small, leading to fluctuations when calculating the coefficient of flexural anisotropy. Next, compared to the control group without added rubber, the experimental group with added rubber shows a decrease in the coefficient of flexural anisotropy, primarily due to the overall reduction in flexural strength. This effect is less pronounced in experimental groups with different rubber content levels. Lastly, the random distribution of rubber and its varying dispersion within the mix can cause fluctuations in the coefficient of flexural anisotropy.

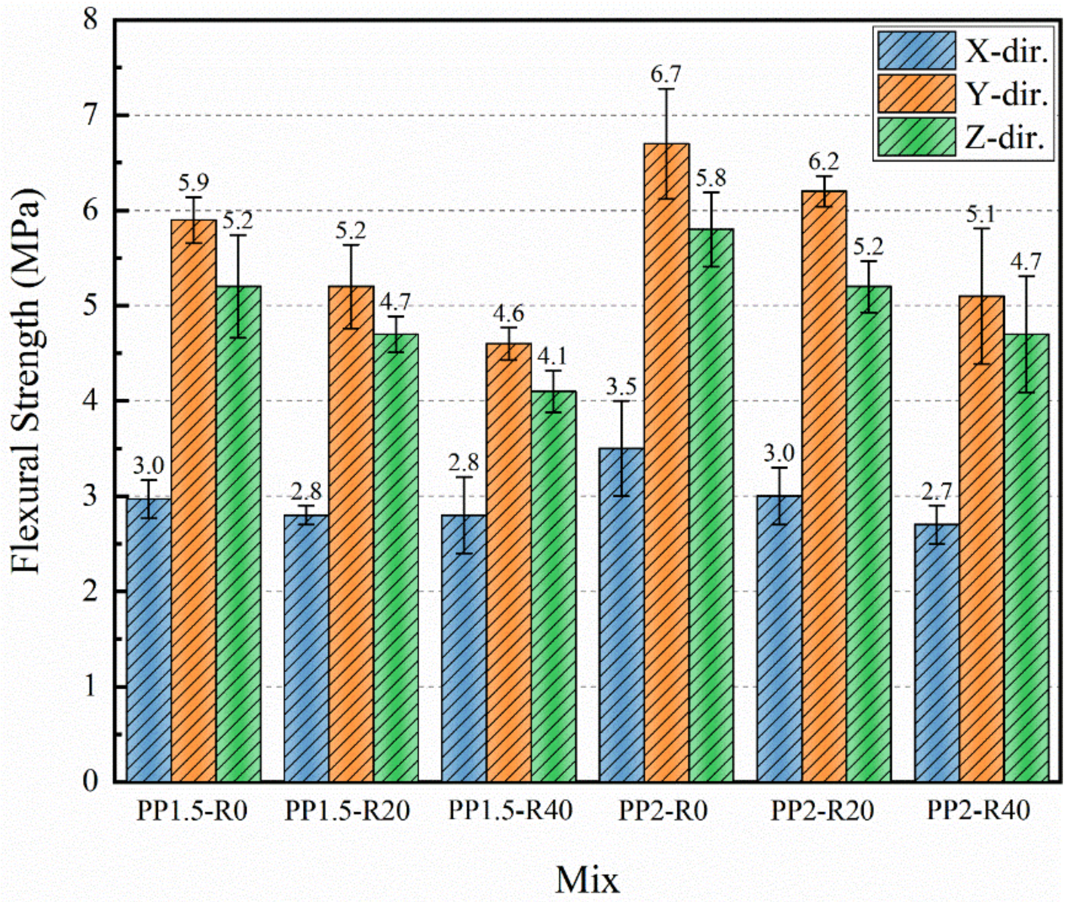

Figure 14: Flexural test results

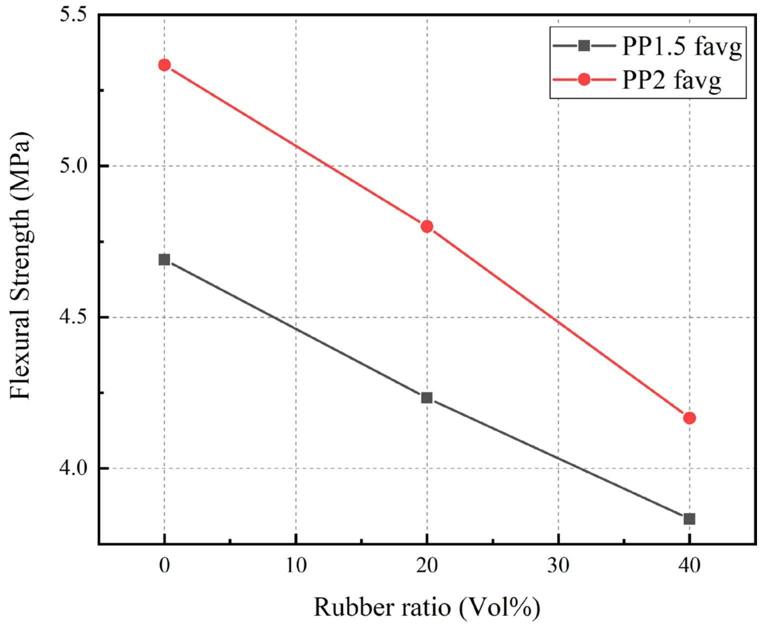

Figure 15: Average flexural strength with the escalating content of rubber

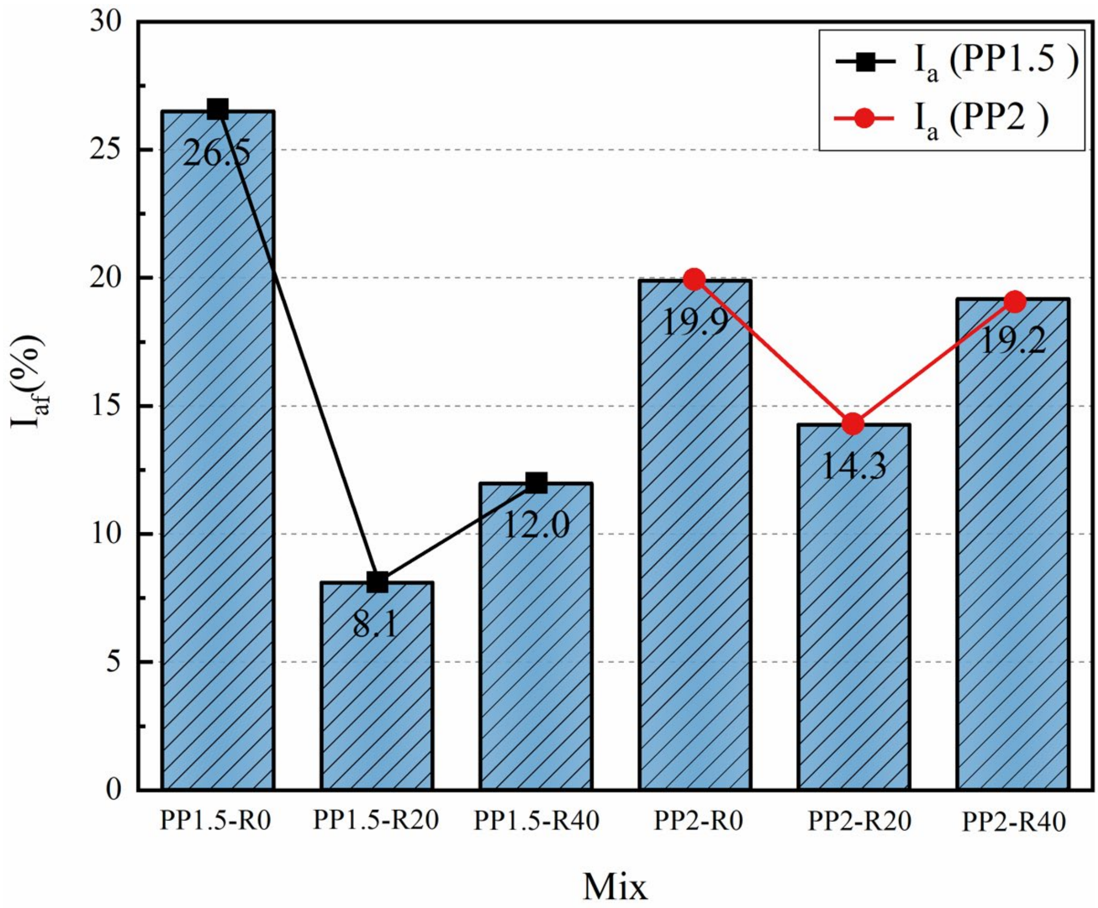

Figure 16: Coefficient of flexural anisotropy (I_{af})

3.4 Global warming potential analysis

Figure 17 shows the normalisation results for four environmental impact indicators for 1 m^3 of concrete using OpenLCA software, presented in a unified unit (year). The concrete production process significantly impacts abiotic depletion (ADP), global warming potential (GWP), and acidification potential (AP). Among these, the most significant impact is global warming, while the smallest is AP. Among the different concrete mix designs, Mix PP2-R0 exhibits the highest ADP, AP, and GWP, which is expected due to the CO_2 emissions released during Portland cement and PP fibre production, contributing to GWP and AP. Waste rubber was managed as municipal waste, and its reuse contributed to the reduction of harmful solid waste incineration, thereby benefiting the environment. Based on the Ecoinvent database, this waste is processed in a municipal solid waste incinerator (MSWI). The proportion of CO_2 emissions for each material within the six mixtures is shown in Figure 18, highlighting cement as the major contributor, accounting for 63% to 83% of GWP. Consistent with findings from other studies (Akbar and Liew 2020; Shobeiri et al. 2021), Figure 18 demonstrates a 28% reduction in GWP when 40% of sand is replaced with waste rubber, confirming the environmental benefits of recycling waste rubber in concrete. The negative GWP values for rubberised mixes indicate environmental credits, justified by offsetting emissions from tire grinding against savings from not producing synthetic rubber (El-Seidy et al. 2022).

Han et al.'s research highlights that material production stages have much higher potential impacts on global warming than the construction stage for both conventional concrete and 3DCP (Han et al. 2021). Weng et al.'s findings suggest that 3D-printed structures can emit up to 85.9% less CO_2 than precast constructions due to reduced formwork usage. However, if formwork is reused over 25 times, the environmental impact of precast and 3D printed constructions becomes comparable (Weng et al. 2020). Thus, the GWP impacts of 3DPC construction should be considered case by case rather than broadly.

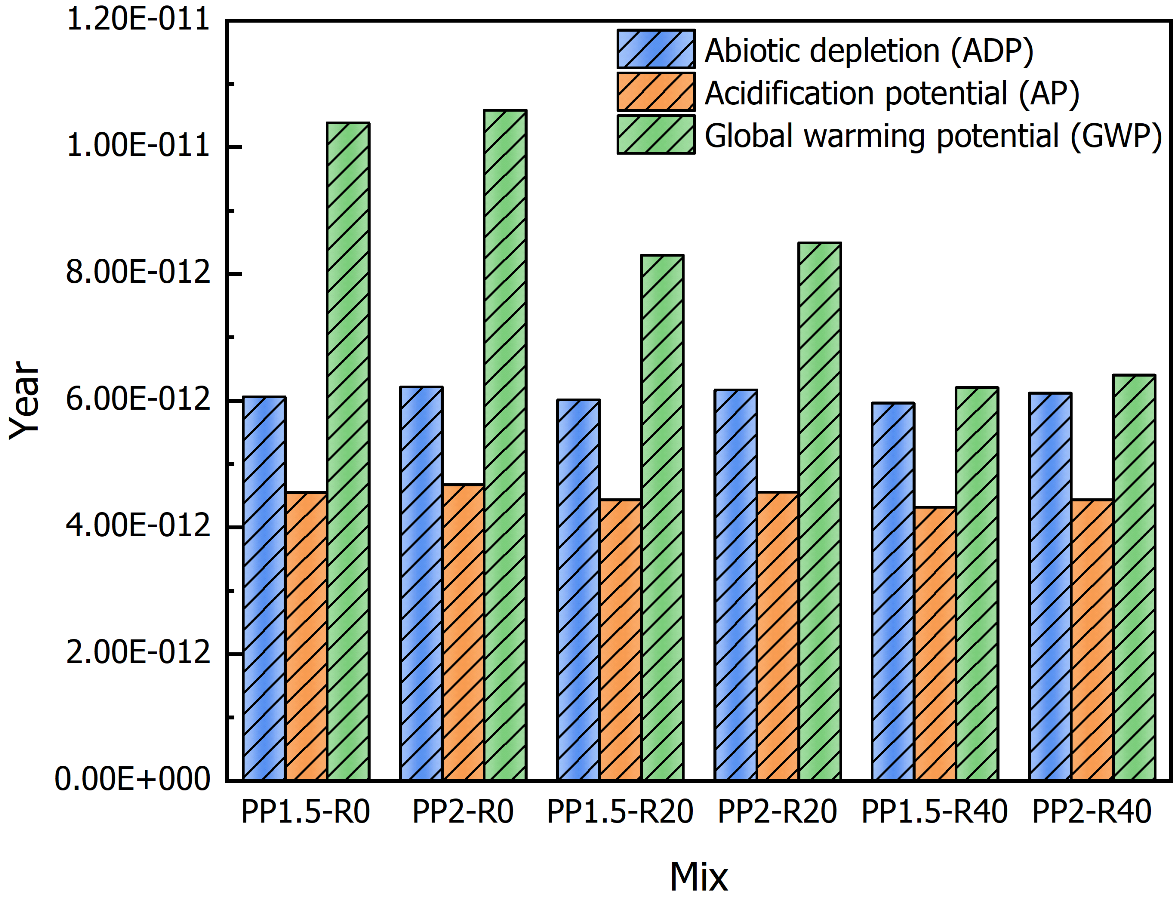

Figure 17: Normalised environmental impact of mixtures.

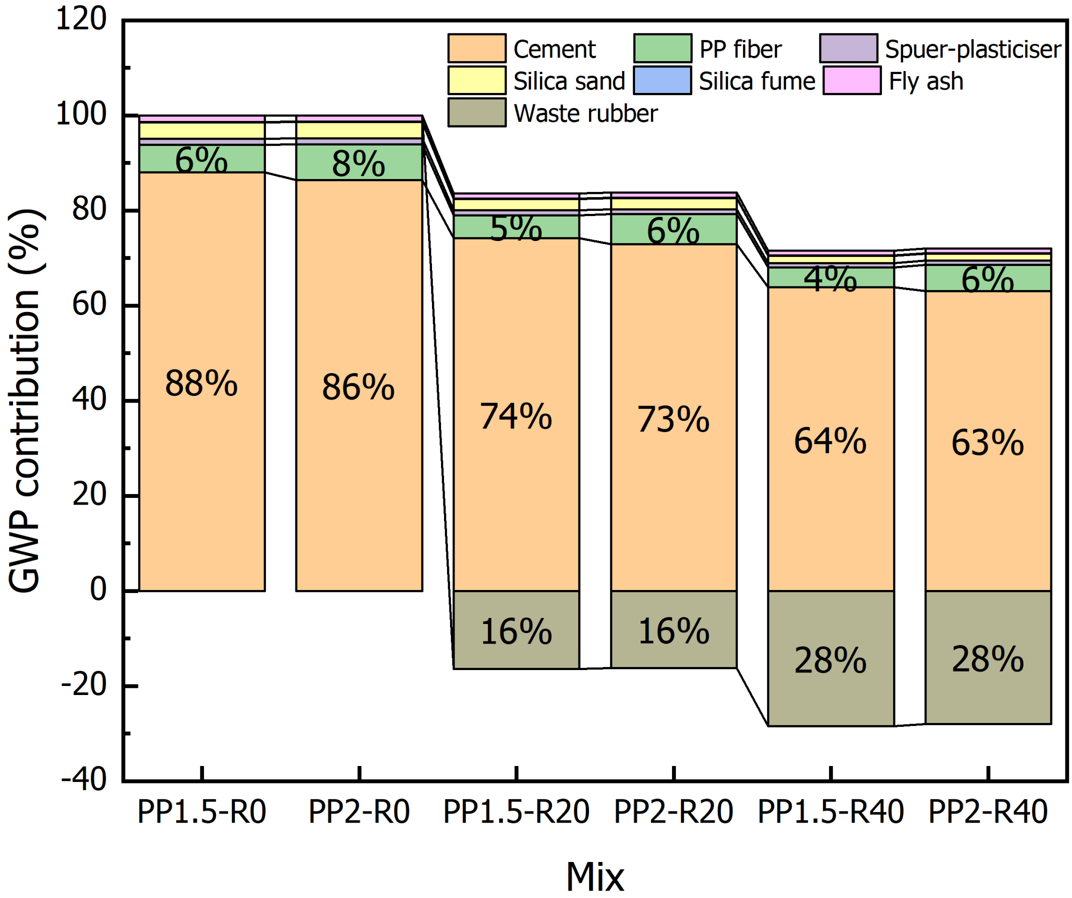

Figure 18: Normalised GWP contribution of mixtures.

4. Conclusion

In this study, a comprehensive examination was conducted of adding rubber particles to the fresh and hardened properties of 3D printable concrete with PP fibres. The key conclusions from the experimental results are as follows:

1. RP enhances the flowability of 3D-printable concrete due to its texture and water absorption properties, while PP fibres decrease it by raising viscosity and friction. Optimal flow is found with 1.5% PP and 40% RP.
2. Compressive test results from six mixtures show that concrete's mechanical properties vary based on loading direction. Maximum compressive strength is observed in the FX loading direction, with the Z direction showing the weakest properties. The introduction of rubber generally reduces compressive strength. The anisotropy coefficient decreases

with increasing rubber content, reflecting rubber's stress-diffusing properties and its role in mitigating stress concentration. Crack progression, captured using DIC, revealed that rubber inclusion results in gradual failures, with rubber's energy absorption slowing microcrack expansion and enhancing material toughness.

3. Flexural strength results indicate that samples loaded in the Y direction display the highest flexural strength. A decline in flexural strength is observed with increasing rubber content, while an increase in fibre content enhances flexural strength. The anisotropy coefficient verifies that adding rubber does not markedly change the material's directional preference in countering bending loads.
4. Recycling waste rubber in concrete significantly reduces the environmental impact, particularly regarding global warming potential. However, the overall GWP assessment for 3D printing construction needs context-specific evaluations, as the benefits can vary greatly depending on construction practices.

5. Future work

While this study has made strides in understanding the mechanical performance and anisotropic characteristics of rubberized 3D-printed concrete, several avenues remain for further investigation. One area is the pretreatment of rubber particles, which could influence the material's properties and performance. Future studies should explore various pretreatment methods, such as coating rubber particles with cement paste or other substances, to enhance their compatibility with the concrete matrix and improve the overall structural integrity of the printed objects. Additionally, while this study utilized specific percentages of PP fibres and rubber particles, further varying these proportions could provide deeper insights into optimizing the material's mechanical properties. The interplay between flowability, strength, and durability as these proportions change remains critical for future exploration. Furthermore, the application of Finite Element Analysis (FEA) presents a promising opportunity for future work. FEA can offer a more detailed understanding of the material's behaviour under various conditions, providing insights not easily obtainable through empirical tests alone. Implementing FEA would allow for a more nuanced simulation of the 3D printing process and the resulting material characteristics, potentially uncovering optimization strategies for material composition and printing parameters.

References

Abdallah, Sadoon, Mizi Fan, and K. A. Cashell. 2017. 'Bond-slip behaviour of steel fibres in concrete after exposure to elevated temperatures', *Construction and Building Materials*, 140: 542-51.

Akbar, Arslan, and K. M. Liew. 2020. 'Assessing recycling potential of carbon fiber reinforced plastic waste in production of eco-efficient cement-based materials', *Journal of Cleaner Production*, 274.

Alami, Abdul Hai, Abdul Ghani Olabi, Mohamad Ayoub, Haya Aljaghoub, Shamma Alasad, and Mohammad Ali Abdelkareem. 2023. '3D Concrete Printing: Recent Progress, Applications, Challenges, and Role in Achieving Sustainable Development Goals', *Buildings*, 13.

Alsaif, Abdulaziz, Lampros Koutas, Susan A. Bernal, Maurizio Guadagnini, and Kypros Pilakoutas. 2018. 'Mechanical performance of steel fibre reinforced rubberised concrete for flexible concrete pavements', *Construction and Building Materials*, 172: 533-43.

Alyousef, Rayed. 2021. 'Sustainable Use of Waste Polypropylene Fibres to Enhance the Abrasion and Skid Resistance of Two-Stage Concrete', *Sustainability*, 13.

Antarvedi, Bhawani, Nawal Kishor Banjara, and Suvir Singh. 2023. 'Optimisation of polypropylene and steel fibres for the enhancement of mechanical properties of fibre-reinforced concrete', *Asian Journal of Civil Engineering*, 24: 1055-75.

Atahan, Ali O., and Ayhan Öner Yücel. 2012. 'Crumb rubber in concrete: Static and dynamic evaluation', *Construction and Building Materials*, 36: 617-22.

Australia, Standards. 2000. "AS 1012.11." In *Methods of testing concrete Determination of the modulus of rupture (Reconfirmed 2014)*.

———. 2014. "AS 1012.9:2014." In *Methods of testing concrete Compressive strength tests - Concrete, mortar and grout specimens*.

Behfarnia, Kiachehr, and Omid Farshadfar. 2013. 'The effects of pozzolanic binders and polypropylene fibers on durability of SCC to magnesium sulfate attack', *Construction and Building Materials*, 38: 64-71.

Chen, Mingxu, Laibo Li, Jiaao Wang, Yongbo Huang, Shoude Wang, Piqi Zhao, Lingchao Lu, and Xin Cheng. 2020. 'Rheological parameters and building time of 3D printing sulphoaluminate cement paste modified by retarder and diatomite', *Construction and Building Materials*, 234.

Chengxiu Jia, Xuhong Qiang, Xu Jiang. 2022. "Comparative Analysis of Carbon Emission of Special-Shaped

Concrete Pier Constructed by 3D Printing and Traditional Construction." In *IABSE Congress: Bridges and Structures: Connection, Integration and Harmonisation, Nanjing, People's Republic of China, 21-23 September 2022*, 2016-23. IABSE Congress Nanjing 2022.

Ding, Maoting, Feng Zhang, Xianzhang Ling, and Bo Lin. 2018. 'Effects of freeze-thaw cycles on mechanical properties of polypropylene Fiber and cement stabilized clay', *Cold Regions Science and Technology*, 154: 155-65.

El-Seidy, Eslam, Matteo Sambucci, Mehdi Chougan, Mazen J. Al-Kheetan, Ilario Biblioteca, Marco Valente, and Seyed Hamidreza Ghaffar. 2022. 'Mechanical and physical characteristics of alkali- activated mortars incorporated with recycled polyvinyl chloride and rubber aggregates', *Journal of Building Engineering*, 60.

Elchalakani, Mohamed. 2015. 'High strength rubberized concrete containing silica fume for the construction of sustainable road side barriers', *Structures*, 1: 20-38.

Feng, Wanhui, Yufei Wang, Junbo Sun, Yunchao Tang, Dongxiao Wu, Zhiwei Jiang, Jianqun Wang, and Xiangyu Wang. 2022. 'Prediction of thermo-mechanical properties of rubber-modified recycled aggregate concrete', *Construction and Building Materials*, 318: 125970.

'GB/T2419-2005, Chinese Standards, Test Method for Fluidity of Cement Mortar, Chinese Standards Association, China, 2005.'.

Gerges, Najib N., Camille A. Issa, and Samer A. Fawaz. 2018. 'Rubber concrete: Mechanical and dynamical properties', *Case Studies in Construction Materials*, 9.

Gesoglu, Mehmet, Erhan Güneyisi, Guler Fakhraddin Muhyaddin, and Diler Sabah Asaad. 2016. 'Strain hardening ultra-high performance fiber reinforced cementitious composites: Effect of fiber type and concentration', *Composites Part B: Engineering*, 103: 74-83.

Hambach, Manuel, and Dirk Volkmer. 2017. 'Properties of 3D-printed fiber-reinforced Portland cement paste', *Cement and Concrete Composites*, 79: 62-70.

Han, Yilong, Zhihan Yang, Tao Ding, and Jianzhuang Xiao. 2021. 'Environmental and economic assessment on 3D printed buildings with recycled concrete', *Journal of Cleaner Production*, 278.

He, Haijie, Hongxia Qiao, Tianying Sun, Haiming Yang, and Chuang He. 2024. 'Research progress in mechanisms, influence factors and improvement routes of chloride binding for cement composites', *Journal of Building Engineering*: 108978 doi: https://doi.org/10.1016/j.jobe.2024.78.

Holmes, Niall, Alex Browne, and Christopher Montague. 2014. 'Acoustic properties of concrete panels with crumb rubber as a fine aggregate replacement', *Construction and Building Materials*, 73: 195-204.

Hossain, F. M. Zahid, Md Shahjalal, Kamrul Islam, Mohammad Tiznobaik, and M. Shahria Alam. 2019. 'Mechanical properties of recycled aggregate concrete containing crumb rubber and polypropylene fiber', *Construction and Building Materials*, 225: 983-96.

ISO, I. S. O. 2006. '14040: 2006 Environmental management-Life cycle assessment-Principles and framework. 2006', *International Organization for Standardization: Geneva*.

Jain, Kranti, and Bichitra Singh Negi. 2021. 'Analysis of steel fibre reinforced concrete beams in flexure: the experimental investigation', *Asian Journal of Civil Engineering*, 22: 1625-37.

Jawad, Zahraa Fakhri, Rusul Jaber Ghayyib, and Awham Jumah Salman. 2020. 'Microstructural and Compressive Strength Analysis for Cement Mortar with Industrial Waste Materials', *Civil Engineering Journal*, 6: 1007-16.

Khan, Sadaqat Ullah, and Tehmina Ayub. 2022. 'Mechanical Properties of Hybrid Self-Compacting Fibre-Reinforced Concrete (SCC-FRC) Containing PVA and PP Fibres', *Iranian Journal of Science and Technology, Transactions of Civil Engineering*, 46: 2677-95.

Lai, Dade, Lan Lin, Xiaoyu Yan, Zitong Li, Keqin Xu, Cristoforo Demartino, and Yan Xiao. 2022. "Development of a

Steel Fiber-Reinforced Rubber Concrete for Jacketing of Bridge Piers Against Vehicular Impacts: Preliminary Results." In, 1144-51. Cham: Springer International Publishing.

Levchenko, A. V., and M. V. Shitikova. 2024. "The Analysis of the Strength Characteristics of Rubber Concrete as Compared with Ordinary Cement Concrete." In, 122-31. Cham: Springer Nature Switzerland.

Liu, Bing, Xiaoyan Liu, Guangtao Li, Songyuan Geng, Zhi Li, Yunhao Weng, and Kai Qian. 2022. 'Study on anisotropy of 3D printing PVA fiber reinforced concrete using destructive and non-destructive testing methods', *Case Studies in Construction Materials*, 17.

Liu, Chao, Jie Cui, Zixin Zhang, Hai Liu, Xin Huang, and Changqiang Zhang. 2021. 'The role of TBM asymmetric tail-grouting on surface settlement in coarse-grained soils of urban area: Field tests and FEA modelling', *Tunnelling and Underground Space Technology*, 111: 103857 doi: https://doi.org/10.1016/j.tust.2021.57.

Liu, Junli, Sujeeva Setunge, and Phuong Tran. 2022. '3D concrete printing with cement-coated recycled crumb rubber: Compressive and microstructural properties', *Construction and Building Materials*, 347.

Liu, Yanzhu, Liang Wang, Ke Cao, and Lei Sun. 2021. 'Review on the Durability of Polypropylene Fibre-Reinforced Concrete', *Advances in Civil Engineering*, 2021: 6652077.

Long, Xu, Ming-hui Mao, Tian-xiong Su, Yu-tai Su, and Meng-ke Tian. 2023. 'Machine learning method to predict dynamic compressive response of concrete-like material at high strain rates', *Defence Technology*, 23: 100-11 doi: https://doi.org/10.1016/j.dt.2022.02.003.

Mohammed, Bashar, and Najwa Azmi. 2011. 'Failure Mode and Modulus Elasticity of Concrete Containing Recycled Tire Rubber', *The Journal of Solid Waste Technology and Management*, 37: 16-24.

Mujalli, Mohammed A., Samir Dirar, Emad Mushtaha, Aseel Hussien, and Aref Maksoud. 2022. 'Evaluation of the Tensile Characteristics and Bond Behaviour of Steel Fibre-Reinforced Concrete: An Overview', *Fibers*, 10.

Najim, Khalid B., and Matthew R. Hall. 2012. 'Mechanical and dynamic properties of self-compacting crumb rubber modified concrete', *Construction and Building Materials*, 27: 521-30.

Nebrida, Jimmy A. 2022. 'Automated Onsite Construction: 3D Printing Technology', *Journal of Engineering Research and Reports*: 47-55.

Nerella, Venkatesh Naidu, Simone Hempel, and Viktor Mechtcherine. 2019. 'Effects of layer-interface properties on mechanical performance of concrete elements produced by extrusion-based 3D-printing', *Construction and Building Materials*, 205: 586-601.

P. Nuaklong, J. Chittanurak, P. Jongvivatsakul, W. Pansuk, A. Lenwari, and S. Likitlersuang. 2020. 'Effect of hybrid polypropylene-steel fibres on strength characteristics of UHPFRC', *Advances in concrete construction*, 10: 1-11.

Pan, Lei, Hong Hao, Jian Cui, and Thong M. Pham. 2022. 'Numerical study on dynamic properties of rubberised concrete with different rubber contents', *Defence Technology*.

Panda, Biranchi A. Shakor Pshtiwan A. Laghi Vittoria. *Additive Manufacturing for Construction*.

Panda, Biranchi, Suvash Chandra Paul, and Ming Jen Tan. 2017. 'Anisotropic mechanical performance of 3D printed fiber reinforced sustainable construction material', *Materials Letters*, 209: 146-49.

Panda, Biranchi, and Ming Jen Tan. 2018. 'Experimental study on mix proportion and fresh properties of fly ash based geopolymer for 3D concrete printing', *Ceramics International*, 44: 10258-65.

Pang, Bo, Heping Zheng, Zuquan Jin, Dongshuai Hou, Yunsheng Zhang, Xiaoyun Song, Yanan Sun, Zhiyong Liu, Wei She, and Lin Yang. 2024. 'Inner superhydrophobic materials based on waste fly ash: microstructural morphology of microetching effects', *Composites Part B: Engineering*, 268 111089 doi: https://doi.org/10.1016/j.compositesb.2023.89.

Petrovic, Vojislav, Juan Vicente Haro Gonzalez, Olga Jordá Ferrando, Javier Delgado Gordillo, Jose Ramón Blasco Puchades, and Luis Portolés Griñan. 2010. 'Additive layered manufacturing: sectors of industrial application shown through case studies', *International Journal of Production Research*, 49: 1061-79.

Pham, Thong M., Mohamed Elchalakani, Hong Hao, Jeffrey Lai, Shaun Ameduri, and Tung M. Tran. 2019. 'Durability characteristics of lightweight rubberized concrete', *Construction and Building Materials*, 224: 584-99.

Pham, Thong M., Mohamed Elchalakani, Ali Karrech, and Hong Hao. 2018. 'Axial impact behavior and energy absorption of rubberized concrete with/without fiber-reinforced polymer confinement', *International Journal of Protective Structures*, 10: 154-73.

Pham, Thong M., X. Zhang, M. Elchalakani, A. Karrech, Hong Hao, and Aarin Ryan. 2018. 'Dynamic response of rubberized concrete columns with and without FRP confinement subjected to lateral impact', *Construction and Building Materials*, 186: 207-18.

Pierce, C. E., and M. C. Blackwell. 2003. 'Potential of scrap tire rubber as lightweight aggregate in flowable fill', *Waste Manag*, 23: 197-208.

Qiu, Jisheng, Min Xing, Zhanlu Yang, Chenghua Zhang, and Xiao Guan. 2020. 'Micro‐pore structure characteristics and macro‐mechanical properties of PP fibre reinforced coal gangue ceramsite concrete', *The Journal of Engineering*, 2020: 1192-97.

Raffoul, Samar, Reyes Garcia, Kypros Pilakoutas, Maurizio Guadagnini, and Nelson Flores Medina. 2016. 'Optimisation of rubberised concrete with high rubber content: An experimental investigation', *Construction and Building Materials*, 124: 391-404.

Rehman, A. U., and J. H. Kim. 2021. '3D Concrete Printing: A Systematic Review of Rheology, Mix Designs, Mechanical, Microstructural, and Durability Characteristics', *Materials (Basel)*, 14.

Saberian, Mohammad, Long Shi, Amir Sidiq, Jie Li, Sujeeva Setunge, and Chun-Qing Li. 2019. 'Recycled concrete aggregate mixed with crumb rubber under elevated temperature', *Construction and Building Materials*, 222: 119-29.

Said, Mohamed, Wael Montaser, Ahmed S. Elgammal, Amr H. Zahir, and Ibrahim G. Shaaban. 2021. 'Shear Strength of Reinforced Mortar Beams Containing Polyvinyl Alcohol Fibre (PVA)', *International Journal of Civil Engineering*, 19: 1155-78.

Sambucci, Matteo, Ilario Biblioteca, and Marco Valente. 2023. 'Life Cycle Assessment (LCA) of 3D Concrete Printing and Casting Processes for Cementitious Materials Incorporating Ground Waste Tire Rubber', *Recycling*, 8.

Shobeiri, Vahid, Bree Bennett, Tianyu Xie, and Phillip Visintin. 2021. 'A comprehensive assessment of the global warming potential of geopolymer concrete', *Journal of Cleaner Production*, 297.

Singh, Amardeep, Zhiyuan Chen, Zhenhua Duan, and Lei Li. 2022. 'Utilization potential of steel fibers in 3D printed functionally graded cementitious composite: An experimental approach', *Materials Letters*, 324.

Singh, Amardeep, Yufei Wang, Yiyi Zhou, Junbo Sun, Xinglong Xu, Yutong Li, Zhonghe Liu, Jing Chen, and Xiangyu Wang. 2023. 'Utilization of antimony tailings in fiber-reinforced 3D printed concrete: A sustainable approach for construction materials', *Construction and Building Materials*, 408: 133689.

Singh, Narinder, Francesco Colangelo, and Ilenia Farina. 2023. 'Sustainable Non-Conventional Concrete 3D Printing—A Review', *Sustainability*, 15.

Strukar, K., T. Kalman Sipos, T. Doksanovic, and H. Rodrigues. 2018. 'Experimental Study of Rubberized Concrete Stress-Strain Behavior for Improving Constitutive Models', *Materials (Basel)*, 11.

Sun, Junbo, Farhad Aslani, Jianjun Wei, and Xiangyu Wang. 2021. 'Electromagnetic absorption of copper fiber oriented composite using 3D printing', *Construction and Building Materials*, 300: 124026.

Sun, Junbo, Sen Lin, Genbao Zhang, Yuantian Sun, Junfei Zhang, Changfu Chen, Amr M Morsy, and Xiangyu Wang. 2021. 'The effect of graphite and slag on electrical and mechanical properties of electrically conductive cementitious composites', *Construction and Building Materials*, 281: 122606.

Sun, Junbo, Weichen Tang, Yufei Wang, Xupei Yao, Bo Huang, Mohamed Saafi, and Xiangyu Wang. 2023.

'Electromagnetic and mechanical performance of 3D printed wave-shaped copper solid superstructures', *Journal of Materials Research and Technology*, 27: 6936-46.

Sun, Junbo, Yunchao Tang, Jianqun Wang, Xiangyu Wang, Jiaqing Wang, Zimei Yu, Qian Cheng, and Yufei Wang. 2022. 'A Multi-objective Optimisation Approach for Activity Excitation of Waste Glass Mortar', *Journal of Materials Research and Technology*.

Sun, Junbo, Xiangyu Wang, Junfei Zhang, Fan Xiao, Yuantian Sun, Zhenhua Ren, Genbao Zhang, Shukui Liu, and Yufei Wang. 2021. 'Multi-objective optimisation of a graphite-slag conductive composite applying a BAS-SVR based model', *Journal of Building Engineering*, 44: 103223.

Sun, Junbo, Yufei Wang, Kefei Li, Xupei Yao, Binrong Zhu, Jiaqing Wang, Qianqian Dong, and Xiangyu Wang. 2022. 'Molecular interfacial properties and engineering performance of conductive fillers in cementitious composites', *Journal of Materials Research and Technology*.

Sun, Junbo, Yufei Wang, Shukui Liu, Ayoub Dehghani, Xiaolei Xiang, Jianjun Wei, and Xiangyu Wang. 2021. 'Mechanical, chemical and hydrothermal activation for waste glass reinforced cement', *Construction and Building Materials*, 301: 124361.

Ul Aleem, Muhammad Ashar, Muhammad Shahid Siddique, Syed Hassan Farooq, Muhammad Usman, Muhammad Hamza Ahsan, Manzoor Hussain, and Asad Hanif. 2022. 'Axial compressive behavior of concrete incorporating crumb rubber pretreated with waste quarry dust', *Journal of Building Engineering*, 59.

Wang, Xianggang, Lutao Jia, Zijian Jia, Chao Zhang, Yuning Chen, Lei Ma, Zhibin Wang, Zhicong Deng, Nemkumar Banthia, and Yamei Zhang. 2022. 'Optimization of 3D printing concrete with coarse aggregate via proper mix design and printing process', *Journal of Building Engineering*, 56.

Weng, Yiwei, Mingyang Li, Shaoqin Ruan, Teck Neng Wong, Ming Jen Tan, Kah Leong Ow Yeong, and Shunzhi Qian. 2020. 'Comparative economic, environmental and productivity assessment of a concrete bathroom unit fabricated through 3D printing and a precast approach', *Journal of Cleaner Production*, 261.

Xiao, Chuang, Ke Zheng, Shenggui Chen, Nan Li, Xin Shang, Feihong Wang, Jiahua Liang, Sadaf Bashir Khan, Yafei Shen, and Bingheng Lu. 2023. 'Additive manufacturing of high solid content lunar regolith simulant paste based on vat photopolymerization and the effect of water addition on paste retention properties', *Additive Manufacturing*, 71: 103607 doi: https://doi.org/10.1016/j.addma.2023.07.

Yang, Senyuan, Yingfan Zhang, Zhou Sha, Zhengyong Huang, Haohuan Wang, Feipeng Wang, and Jian Li. 2022. 'Deterministic manipulation of heat flow via three-dimensional-printed thermal meta-materials for multiple protection of critical components', *ACS Applied Materials & Interfaces*, 14: 39354-63 doi: 10.1021/acsami.2c09602.

Yao, Xiaofei, Xin Lyu, Junbo Sun, Bolin Wang, Yufei Wang, Min Yang, Yao Wei, Mohamed Elchalakani, Danqi Li, and Xiangyu Wang. 2023. 'AI-based performance prediction for 3D-printed concrete considering anisotropy and steam curing condition', *Construction and Building Materials*, 375.

Ye, Junhong, Can Cui, Jiangtao Yu, Kequan Yu, and Fangyuan Dong. 2021. 'Effect of polyethylene fiber content on workability and mechanical-anisotropic properties of 3D printed ultra-high ductile concrete', *Construction and Building Materials*, 281.

Yu, Guofeng, Guanwen Cheng, Lianchong Li, Chunan Tang, Bo Ren, and Yunchun Han. 2020. 'Preliminary Study on High-Energy and Low-Energy Microfracture Event Evolution Characteristics in the Development Process of Rock Failure', *Geofluids*, 2020: 1-17.

Zhou, Tao, Fangzhou Yu, Lingwen Li, Zejiao Dong, and Elham H Fini. 2023. 'Swelling-degradation dynamic evolution behaviors of bio-modified rubberized asphalt under thermal conditions', *Journal of Cleaner Production*, 426: 139061 doi: https://doi.org/10.1016/j.jclepro.2023.61.

Zhu, Binrong, Yufei Wang, Junbo Sun, Yang Wei, Huzi Ye, Hongyu Zhao, and Xiangyu Wang. 2023. 'An experimental study on the influence of waste rubber particles on the compressive, flexural and impact properties of 3D printable sustainable cementitious composites', *Case Studies in Construction Materials*, 19: e02607.

Statements & Declarations

Ethical Approval This research did not involve Human Participants or Animals. Accordingly, ethical approval was not required as per institutional guidelines and national regulations.

Consent to Participate Not applicable, as no human participants were involved in the study.

Consent to Publish The authors affirm that all co-authors have provided their consent to publish this manuscript. The manuscript is original, has not been published previously, nor is it under consideration for publication elsewhere. All the authors have approved the manuscript and agree with its submission to Environmental Science and Pollution Research.

Authors Contributions All authors contributed significantly to the study's conception and design:

- Conceptualization was led by Junbo Sun and Yufei Wang.
- Xin Lyu, Mohamed Elchalakani, and Xiangyu Wang designed the experimental program.
- The experiments were conducted by Xin Lyu and Yufei Wang.
- Data curation was managed by Bo Huang and Mohamed Saafi.
- Formal analysis and investigation were carried out by Junbo Sun and Binrong Zhu.
- Data analysis was performed by Xin Lyu, Mohamed Elchalakani, and Ziqing Wei.
- Xin Lyu and Yufei Wang were responsible for visualization and drafting the initial manuscript.
- Supervision and project administration were handled by Junbo Sun, Binrong Zhu, Bo Huang, and Mohamed Saafi.
- The manuscript was reviewed and edited by Mohamed Elchalakani and Xiangyu Wang.

Funding The authors gratefully acknowledge the financial support from the Road Safety RSIF Grant RSIF-230.

Competing Interests The authors declare no competing financial interests or personal relationships that could have appeared to influence the work reported in this paper.

Availability of data and materials Data and materials are made available on reasonable request.